„New trends in supramolecular chemistry"
Edited by Volodymyr I. Rybachenko
Donetsk 2014, East Publisher House, ISBN 978-966-317-208-8

Chapter 8

Acid-base equilibria in 'oil-in-water' microemulsions. The particular case of fluorescein dyes

Nikolay O. Mchedlov-Petrossyan, Natalya V. Salamanova, and Natalya A. Vodolazkaya
V.N. Karazin Kharkov National University, Svoboda Sq. 4, 61022 Kharkov, Ukraine

1. Introduction

An increasing use of organized solutions in different branches of chemistry [1–13] calls for extending the concepts of ionic equilibria in these media. Lyophilic systems, that is, thermodynamically stable dispersions with well-reproducible properties, are probably most suitable for analytical chemistry and molecular spectroscopy. In addition to typical lyophilic dispersions, such as micellar solutions of colloidal surfactants in water, these systems include microemulsions usually formed by a colloidal surfactant, a hydrocarbon, and an alcohol, which possess limited solubility in water [1, 3, 5, 8, 14].

Protolytic equilibria in microemulsions have been studied less comprehensively than those in micellar solutions of surfactants. The corresponding publications are few in number [13, 15–22], as compared with the vast literature devoted to acid-base reactions in micellar solutions of surfactants. (See, for instance, some reviews [13, 23–25]).

In order to fill up this gap, we decided to gain insight into the properties of microemulsions as media for such processes.

Our previous studies were devoted to determination of the parameters of ionic equilibria of a set of acid-base indicators in microemulsions stabilized by cationic, anionic, and non-ionic surfactants. In these colloidal systems, sulfonephthaleins, azo-dyes and some other common acid-base indicators, as well as solvatochromic Reichardt's betaine dyes have been studied [20–22].

This work was aimed to systematic study of protolytic behavior of three widely used hydroxyxanthene luminophores, namely fluorescein and its 2,4,5,7-tetrabromo- and 2,4,5,7-tetraiodo derivatives (eosin and erythrosin,

respectively), in microemulsions of 'oil-in-water' type. Earlier we have already studied a set of hydroxyxanthene dyes in cationic surfactant-based microemulsions at high ionic strength of the aqueous phase [26, 27] and in reversed AOT-base water-in-oil microemulsions [27–29]. Basing on the results obtained, we have chosen the direct microemulsions 'benzene – pentanol-1 – surfactant – water' based on cationic, anionic, and non-ionic surfactants, under identical conditions. Following surfactants were used: cetyltrimethylammonium bromide, CTAB, sodium *n*-dodecylsulfate, SDS, and non-ionic surfactant Tween 80, TW 80.

Fluorescein dyes are widely used in analytical chemistry and neighboring fields, first of all owing to their unique fluorescent properties. The structure of fluorescein dianion is shown below:

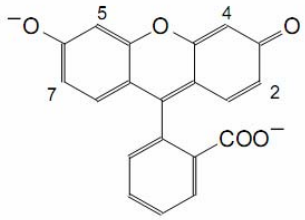

These dyes are applied for optical sensing of O_2, CO_2, H_2S, sulfur-containing organic compounds [30–34], as pH-sensors, including fiber-optical systems [32, 35–37], in biochemistry [38–45], as tracers for hydrological investigations [46]. These compounds are now intensively utilized in nanochemistry [47, 48] and as guest molecules in supramolecular chemistry [49, 50], as fluorescent dyes in molecular beacons [51], for imaging nitric oxide production [52, 53], etc. The spectral and acid-base behavior of the dyes in the presence of surfactants was examined [54, 57]. In some cases, the hydrophobic representatives of this family of dyes, bearing one or two long hydrocarbon chains [25, 42, 54, 55, 57–62], possess some advantages as compared with the parent compounds, e.g., in optical sensors [61], two-phase indicators [58, 59], for studying lyophilic colloidal systems [25, 42, 54, 55, 57, 60], etc. The fluorescent properties of fluorescein and its derivatives are recently used for creation of ratiometric fluorescent pH and temperature probes based on hydrophilic block copolymers [63] and for turn-on fluorescent detection of tartrazine in the presence of graphene oxide [64].

Most often, application of hydroxyxanthenes is connected primarily with embedding them into non-aqueous environments. So far the latter were modeled either by water-organic mixtures, or by micellar solutions of surfactants. In microemulsions, the particle diameter of the dispersed phase is usually larger as compared with common surfactant micelles, and the nanodroplets are considered

as swollen surfactant micelles [14]. Hence, microemulsions can be regarded as a transition step from surfactant micelles to organic solvents. On the other hand, microemulsions can be considered as reduced models of more complex objects, such as suspensions of phospholipid liposomes, polymer films, Langmuir–Blodgett multilayers, and sol-gel systems doped by surfactants.

Throughout the last decade, hydroxyxanthene dyes have been increasingly utilized in organic solvents. Thus, fluorescein was proposed for oxygen and carbon dioxide monitoring in dimethylformamide and dimethylsulfoxide solutions [30, 65]; some new studies are devoted to fluorescence lifetimes of fluorescein dianion [66] and to spectral properties of fluorescein monoanion [39] in organic media. Consequently, a further development of knowledge about the influence of non-aqueous media on the interconversions of the various prototropic forms of these substances is necessary.

The study of protolytic equilibria and visible spectra of organic dyes is a touchstone for research of the influence of microenvironment on the properties and reactivity of these substances. Acid-base ionization of fluorescein dyes in solution occurs stepwise [24, 26–29, 67–70]:

$$H_3R^+ \rightleftharpoons H_2R + H^+, \; K_{a0} \qquad (1)$$

$$H_2R \rightleftharpoons HR^- + H^+, \; K_{a1} \qquad (2)$$

$$HR^- \rightleftharpoons R^{2-} + H^+, \; K_{a2} \qquad (3)$$

The detailed scheme of protolytic equilibria includes several tautomers of molecules and monoanions (Fig. 1). The most intensive absorption and fluorescence in the visible portion of the spectrum possesses the dianion **7**, and (in the case of substances with electron-acceptor substituents in the xanthene nuclei) also the monoanion **6b**,**c**. The latter tautomer is atypical for the parent compound fluorescein, but some traces of species **6a** may be detected in non-hydrogen bond donor solvents [70]. Until now, mono- and dianions possessing lactonic structures are detected only in the case of nitro-substituted fluoresceins, e.g., for 2,4,5,7-tetranitrofluorescein [69].

Previously we have studied the protolytic equilibria of fluorescein and its derivatives in micellar solutions of surfactants [60, 71–74], in solutions of water-soluble dendrimers [75], in aqueous dispersions of CTAB-modified silica nanoparticles [76], in Langmuir–Blodgett films [77], and in aqueous solutions in the presence of β-cyclodextrin [78] and cationic calixarenes [79, 80].

A comparison of the obtained results with the parameters of protolytic

equilibrium in water and micellar solutions of the corresponding surfactants will enable us to predict the effect of microemulsions on organic reagents, which will provide a more rational use of this type of organized solutions in analytical chemistry.

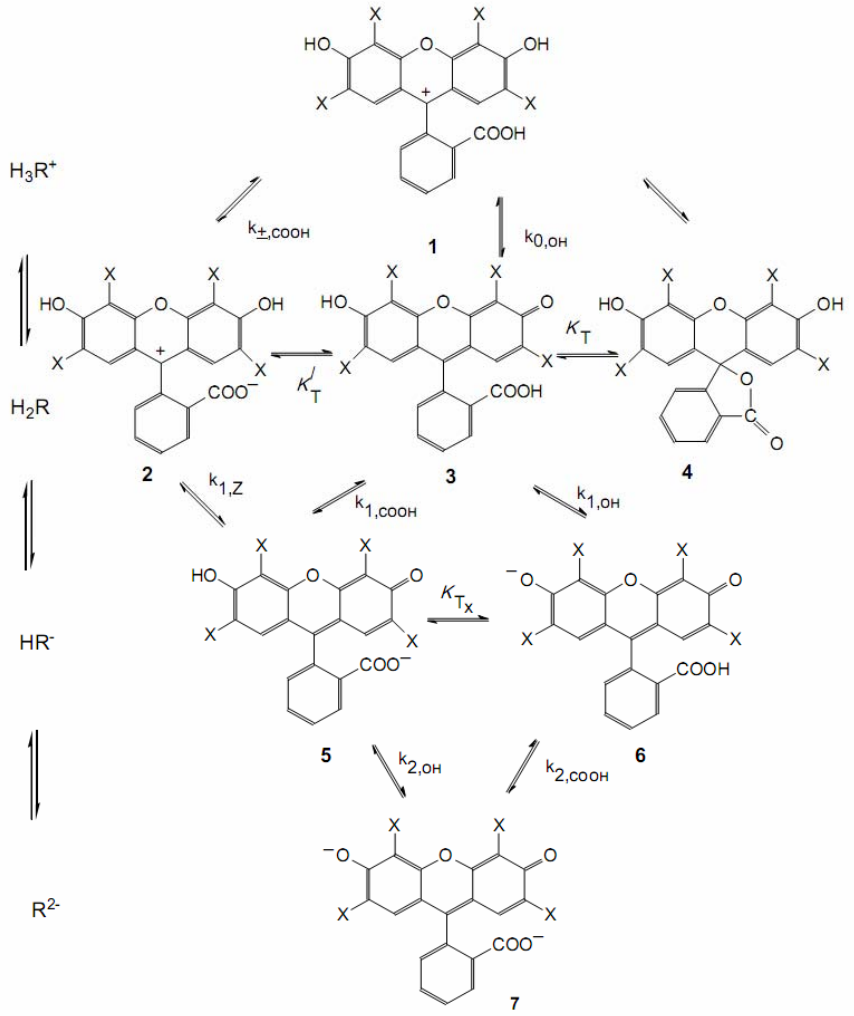

Figure 1. Protolytic conversions of hydroxyxanthenes; fluorescein (X = H): ***1a-7a****, 2,4.5,7-tetrabromofluorescein (eosin) (X = Br):* ***1b-7b****, and 2,4,5,7-tetraiodofluorescein (erythrosin) (X = I):* ***1c-7c***

$K_T = a_4/a_3$; $K'_T = a_2/a_3$; $K''_T = K_T / K'_T = a_4/a_2$; $K_{T_x} = a_6/a_5$; $k_{\pm,COOH} = ha_2 / a_1$; $k_{0,OH} = ha_3 / a_1$; $k_{1,Z} = ha_5 / a_2$; $k_{1,COOH} = ha_5 / a_3$; $k_{1,OH} = ha_6 / a_3$; $k_{2,OH} = ha_7 / a_5$; $k_{2,COOH} = ha_7 / a_6$.

A key characteristic of an indicator in organized solutions is the so-called 'apparent' ionization constant, K_a^{app} [13, 20–26, 71–74]:

$$pK_a^{app} = pH + \log\{[HB^z]/[B^{z-1}]\} \quad (4)$$

Here z and (z–1) are charges of the conjugated indicator species ($HB^z \rightleftharpoons B^{z-1} + H^+$). We define the corresponding K_a^{app} constant as $K_{a(1-z)}^{app}$. The ratio of the equilibrium concentrations of these species can be derived from electronic absorption, while the pH values of the bulk (continuous, aqueous) phase are determined as a rule by using the glass electrode in a cell with liquid junction.

2. Experimental

2.1. Materials

The samples of xanthene dyes used in the present study were purified by re-precipitation or/and by column chromatography. Their purity was checked previously [26, 28, 29, 67, 68], and was additionally controlled by fluorescence excitation spectra of their aqueous alkaline solutions. Phosphoric and hydrochloric acids and potassium chloride were of analytical grade, stock CH_3COOH solutions were prepared from glacial acetic acid, the sample of sodium tetraborate was twice re-crystallized. The stock NaOH solution, prepared from saturated carbonate-free sodium hydroxide solution using CO_2-free water, was kept protected from atmosphere and standardized using potassium biphthalate. CTAB (99 % purity) and TW 80 were from Sigma, the sample of SDS (98.1 % purity) was from Merck. Organic solvents were of analytical grade. Pentanol-1 was purified by standard procedure; the absence of aldehydes was checked by the UV-spectra.

2.2. Apparatus

Absorption spectra of dye solutions were measured using SF-46 apparatus (Russia), with optical path length l = 1 to 5 cm. The absorbance of reference solutions containing all the components except dyes was close to that of water. Fluorescence spectra were registered by Hitachi F 4010 fluorometer in the Laboratory of Professor A. O. Doroshenko, Kharkov National University. The results of zeta-potential determinations mentioned in this paper were obtained by Dr. L. V. Kutuzova in the Laboratory of Professor M. Ballauff, University of Bayreuth, Germany, as described previously [76, 79, 80]. The pH measurements of the bulk (aqueous) phase were performed at 25.0 ± 0.1^0C on a P 37-1 potentiometer and pH-121 pH-meter equipped with ESL-63-07 glass electrode

reversible to H^+ ions and an Ag/AgCl reference electrode in a cell with liquid junction (1 M KCl). Standard buffer solutions (pH 1.68, 4.01, 6.86, and 9.18) were used for cell calibration. The experimental uncertainty in the measured pH value did not exceed 0.02 pH unit (standard deviation).

2.2. Procedure

Stock microemulsions based on cationic surfactant were prepared by mixing 0.0047 mole of CTAB or CPC with 2.3 ml of pentanol-1, then 0.43 cm^3 of benzene and, finally, 5.5 cm^3 of H_2O were added [21, 22]. In the case of anionic microemulsions, 1.417 g of SDS were mixed with 3.46 cm^3 of alcohol, then 1.87 cm^3 of benzene and 22.7 cm^3 of H_2O were added; in the case of non-ionic microemulsions, the above quantities were as follows: 14.65 g (TW 80), 5.1 cm^3 (pentanol-1), 2.0 cm^3 (C_6H_6), and 11.85 cm^3 (H_2O) [21]. Working solutions were prepared by dilution of stock solutions with water, with addition of buffer components and aliquots of stock dye solutions, and made up to required volume at 25 °C. The volume fraction, φ, of organic phase in working solutions was calculated taking into account the amount of water in the stock microemulsion.

The pH values were varied as a rule applying buffer solutions. Acetate and phosphate buffer solutions were obtained by mixing required amounts of the stock acid solutions and the standard NaOH solution. Borax was used for creating higher pH values. The HCl solutions were used at pH < 3.5 and diluted NaOH at pH around 12. In all the cases, the ionic strength of aqueous solutions, I, was maintained constant (= 0.05 M) by additions of calculated amounts of KCl. Only at pH below 1.3, the ionic strength was higher, especially in the case of fluorescein.

The pK_a^{app} values were determined at $\varphi = 0.013$ vis-spectroscopically by the standard procedure [13, 20–29, 60, 71–74]. The systems under study contained 4.9 mole of pentanol-1 and 1 mole of benzene per 1 mole of CTAB, 9.3 mol of pentanol-1 and 2 mole of benzene per 1 mole of TW 80, and 6.5 and 4.3 mole of pentanol-1 and benzene per 1 mole of SDS, respectively; this corresponds to the stability region of the studied microemulsions [21, 22].

Stock aqueous solutions of dyes were prepared with small addition of NaOH. The working concentrations of dyes, C, were as a rule (6 to 20)$\times 10^{-6}$ M during pK_a^{app} determination and (3–4)$\times 10^{-6}$ M at emission spectra measurements; in the case of fluorescein the H_2R spectra were measured at dye concentration 2×10^{-5} M.

The instrumental pH values of aqueous buffer solutions as a rule stay practically unchanged after organic phase adding; alterations observed in some cases are, probably, due to the partial binding of the buffer components by the

nanodroplets. However, from our previous studies it follows that in these cases the determined values of pK_a^a of indicators insignificantly differ from those obtained in other buffer systems [81]. Hence, the indicator ratio demonstrates stable response to the bulk pH value.

3. Results and discussion

3.1. Determination of apparent ionization constants

The pK_a^{app} values of the three dyes are determined in each of the three colloidal systems. Several representative pH-dependences of absorbances are depicted in Figure 2.

The stepwise ionization constants are calculated by using the dependences of *A vs.* pH at a fixed wave length and constant total dye concentration and optical path [Eq. (5)]:

$$A = \frac{A_{H_3R^+} h^3 + A_{H_2R} h^2 K_{a0}^{app} + A_{HR^-} h K_{a0}^{app} K_{a1}^{app} + A_{R^{2-}} K_{a0}^{app} K_{a1}^{app} K_{a2}^{app}}{h^3 + h^2 K_{a0}^{app} + h K_{a0}^{app} K_{a1}^{app} + K_{a0}^{app} K_{a1}^{app} K_{a2}^{app}} \qquad (5)$$

Here A is the absorbance at the current pH value, $A_{R^{2-}}$, A_{HR^-}, A_{H_2R} and $A_{H_3R^+}$ are absorbances under conditions of complete conversion of the dye into the corresponding form, $h \equiv 10^{-pH}$. In the case of eosin and erythrosin, the pK_{a0}^{app} values lie in the far acidic region and are not determined here, and hence it is possible to simplify Eq. (5). Moreover, for fluorescein in cationic and non-ionic microemulsions, the pK_{a0}^{app} value can be estimated separately from pK_{a1}^{app} and pK_{a2}^{app}. For calculations of the pK_{a1}^{app} and pK_{a2}^{app} values of a dye in a given system, at least 15 solutions with various pH values at $I = 0.05$ M and not less than 12 wavelengths within the visible region are used. For determination of pK_{a0}^{app} value of fluorescein in non-ionic microemulsion, working solutions pH values within the range 1.30–2.40 are utilized; 4 wavelengths in the region of λ_{max} of cationic species, H_3R^+, are used as analytical positions. The spectra at HCl concentrations 2 M and 3 M coincide, which allows regarding their absorbances as $A_{H_3R^+}$ values. In cationic microemulsions, the interval of working pH was 1.29–1.85; $I = 0.05$ M. And again, the spectrum of H_3R^+ species was obtained at high hydrochloride concentrations: the spectra of fluorescein at 2.0 M and 4.0 M of HCl coincide.

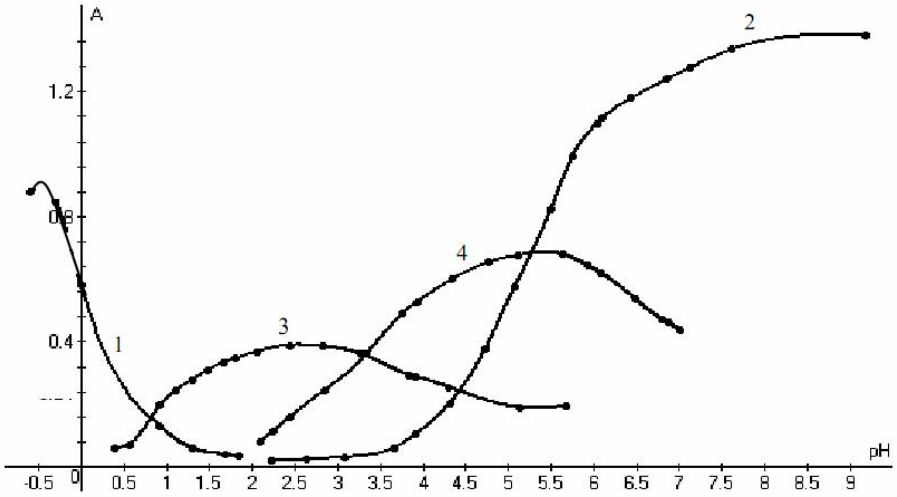

Figure 2. Plots of absorbance against pH: 1 – fluorescein, C = 2.03×10⁻⁵ M, λ = 440 nm, 2– fluorescein, C = 2.03×10⁻⁵ M, λ = 490 nm, 3 – eosin, C = 5.94×10⁻⁶ M, λ = 540 nm, 4 – erythrosin, C = 7.56×10⁻⁶ M, λ = 550 nm; curves 1-3: microemulsions with CTAB, curve 4 – microemulsion with TW 80; all the data are re-calculated to optical path length 1 cm.

In a general case, the A_{HR^-} values are unavailable for direct measurements and are to be calculated jointly with the pK_a^{app} values. The $A_{R^{2-}}$ values and first approximation of A_{H_2R} values are obtained directly at suitable pH. The calculations were carried out using the CLINP program [82]. The pK_a^{app} values are presented in Table 1.

3.2. The treatment of apparent ionization constants: electrostatic approach

The differences between apparent value in micellar solution or in microemulsion, pK_a^{app}, and the 'aqueous' value, pK_a^w, of the same indicator can be explained in terms of electrostatic theory [13, 24, 25].

The pK_a^{app} value of the indicator couple HB^z/B^{z-1} depends on the electrostatic surface potential Ψ of nanodroplets and on other equilibrium parameters [Eq. (6)]:

$$pK_a^{app} = pK_a^w + \log\frac{\gamma_B}{\gamma_{HB}} + \log\frac{f_B^m}{f_{HB}^m} - \frac{\Psi F}{2.303RT} - \log\frac{1+P_B^{-1}(\varphi^{-1}-1)}{1+P_{HB}^{-1}(\varphi^{-1}-1)} \qquad (6)$$

Here pK_a^w is the thermodynamic value of pK_a in water, γ_i are the transfer activity coefficients of the corresponding species from water to the pseudophase, f_i^m are the concentration activity coefficients of the species bound by the pseudophase, Ψ is the electrical potential of the Stern layer, F is the Faraday constant, R is the gas constant, and T is absolute temperature. At $T = 298.15$ K, $2.303RT/F = 59.16$ mV.

Table 1. Indices of the apparent ionization constants values of hydroxyxanthene dyes in microemulsions; $\varphi = 0.013$, $I = 0.05$ M, 25 °C.

Fluorescein			Eosin		Erythrosin	
pK_{a0}^{app}	pK_{a1}^{app}	pK_{a2}^{app}	pK_{a1}^{app}	pK_{a2}^{app}	pK_{a1}^{app}	pK_{a2}^{app}
Benzene – *n*-$C_5H_{11}OH$ –CTAB						
–0.03 ± 0.04[a]	4.49 ± 0.03[a]	5.62 ± 0.08[a]	1.14 ± 0.08	3.69 ± 0.06	1.60 ± 0.07	4.03 ± 0.08
Benzene – *n*-$C_5H_{11}OH$ –TW 80						
0.31 ± 0.07	6.46 ± 0.06	7.08 ± 0.04	3.64 ± 0.07	6.17 ± 0.04	3.47 ± 0.05	6.44 ± 0.04
Benzene – *n*-$C_5H_{11}OH$ – SDS						
2.61 ± 0.04	5.53 ± 0.14	6.62 ± 0.07	3.57 ± 0.10	5.15 ± 0.10	4.41 ± 0.10	5.48 ± 0.10
None (water, $I = 0.05$ M)						
2.22[b]	4.37[b]	6.55[b]	2.73[b]	3.50[b]	≈ 3.8[b]	≈ 4.8[b]

[a] *In analogous system, with CPC instead of CTAB,* $pK_{a0}^{app} = 0.19 \pm 0.03$, $pK_{a1}^{app} = 4.34 \pm 0.02$, $pK_{a2}^{app} = 5.51 \pm 0.04$ *[83].* [b] *From ref. [29].*

The ratio of the bulk (aqueous) and dispersed phases, v_w / v_m, is equal to $(\varphi^{-1} - 1)$. Taking into account high electrolyte concentration in the Stern layer, it is reasonable to regard the ratio f_B^m / f_{HB}^m as being close to unity [13, 24, 25]. The P_i are the partition constants of the corresponding species, *i*, between the bulk phase and the pseudophase. Thermodynamic P_i value is equal to the ratio of activities in corresponding phases ($P_i = a_i^m / a_i^w$). Taking into account the (possible) charge of the dye species the electrical potential of the nanodroplet/ water interface, one obtains the following expression:

$$P_i = \gamma_i^{-1} \, e^{-z_i \Psi F / RT} \qquad (7)$$

The value of the interfacial charge of the pseudophase is substantial. So, for the SDS-based system, the zeta-potential was estimated as $\zeta = -66 \pm 3$ mV;

for the earlier studied system benzene – *n*-pentanol – CPC [21, 22, 83, 84], ζ = +25 ± 5 mV. The size of the droplets in these two dispersions appeared to be surprisingly small, 4.4 and 4.85 nm, respectively, while for microemulsions of *n*-hexane, stabilized by *n*-pentanol and a non-ionic surfactant Triton X-100, the diameters are 9.6 and 16.6 nm for φ = 0.013 and 0.129, respectively. (All data were determined in the presence 0.05 M NaCl.)

From Eq. (6) it is evident that the values ($\Delta pK_a^{app} = pK_a^{app} - pK_a^{w}$) in the given dye/microemulsion system depend on the completeness of binding and on the solvation character of bound species in the pseudophase. In the expression for the apparent pK_a^{app} value under conditions of practically complete binding of the indicator couple HB^z/B^{z-1}, the last logarithmic term in Eq. (6) disappears.

3.3. Vis spectra of ionic and molecular species: structure and tautomerism

Having the K_{a1}^{app} and K_{a2}^{app} values (Table 1) made it possible to calculate the absorbances of HR^- ions at various wavelengths, and in such way to obtain the spectra of these species [Eq. (8)]:

$$A_{HR^-} = A + (A - A_{H_2R})h(K_{a1}^{app})^{-1} + (A - A_{R^{2-}})h^{-1}K_{a2}^{app} \quad , \qquad (8)$$

where A is absorbance at the current pH value. The interval $pK_{a1}^{app} \le pH \le pK_{a2}^{app}$ is used. The A_{HR^-} values, obtained jointly with the K_{a1}^{app} at analytical wavelength, are refined in the same manner. The ε_{HR^-} values are calculated using the A_{HR^-} values: $\varepsilon_{HR^-} = A_{HR^-}\, l^{-1}\, C^{-1}$.

The A_{H_2R} values are, in turn, calculated by using Eq. (7), in order to avoid any influence of traces of intensely colored ions (H_3R^+, HR^- and R^{2-}) on the spectra of the neutral forms:

$$A_{H_2R} = A + (A - A_{H_3R^+})hK_{a0}^{app\,-1} + (A - A_{HR^-})h^{-1}K_{a1}^{app} \, . \qquad (9)$$

The molar absorptivities of neutral species are calculated as $\varepsilon_{H_2R} = A_{H_2R}\, l^{-1}\, C^{-1}$. The spectra of individual ionic and molecular species of fluorescein, singled out in such manner, are typified in Figures 3–5. The λ_{max} values of hydroxyxanthene ions in microemulsions are compiled in Table 2.

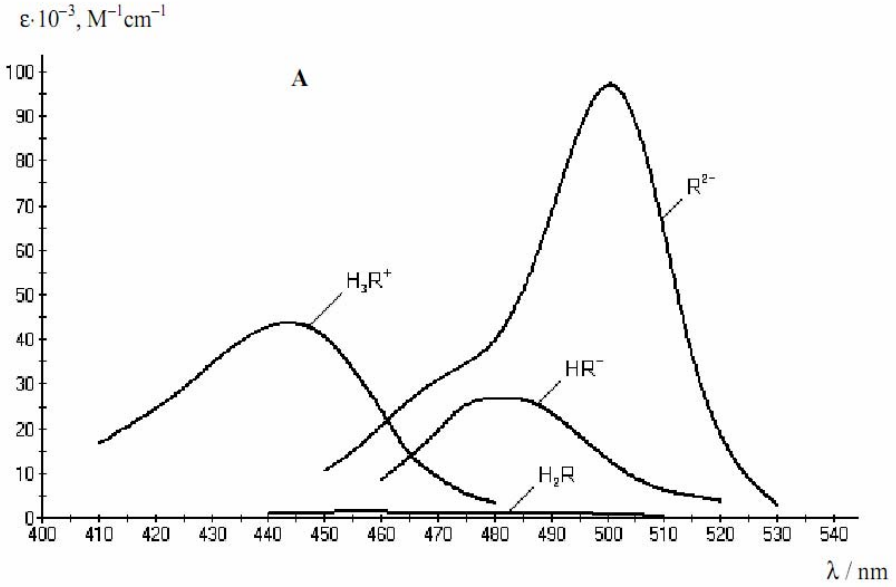

Figure 3. The absorption spectra of the equilibrium forms of fluorescein in the CTAB-based microemulsion.

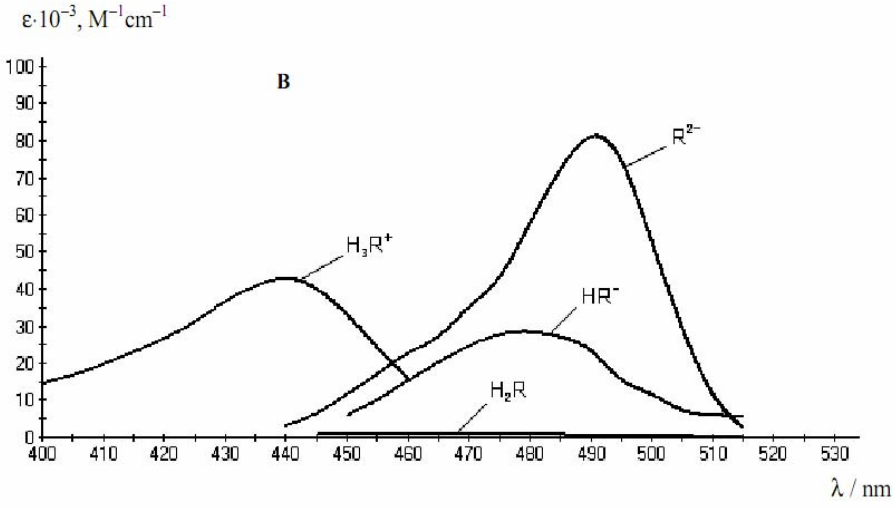

Figure 4. The absorption spectra of the equilibrium forms of fluorescein in the TW 80 based microemulsion.

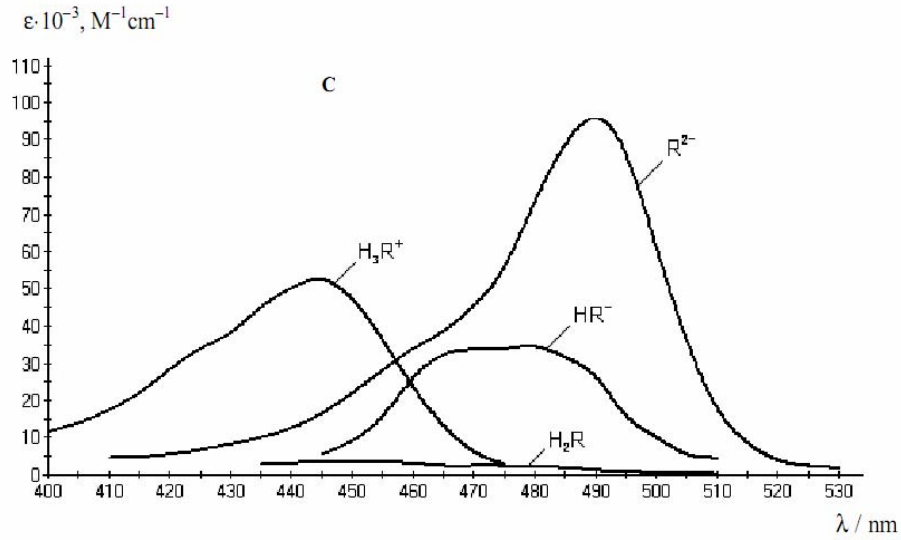

Figure 5. The absorption spectra of the equilibrium forms of fluorescein in the SDS-based microemulsion.

Table 2. The λ_{max}*/nm values of hydroxyxanthene ions in microemulsions;* φ *= 0.013.*

	Water	Microemulsions		
		Benzene – n-$C_5H_{11}OH$ – CTAB	Benzene – n-$C_5H_{11}OH$ – TW 80	Benzene – n-$C_5H_{11}OH$ – SDS
Fluorescein, H_3R^+	437	440	440	445
HR^-	455, 475	480	480	480
R^{2-}	490	500	490	490
Eosin, HR^-	517–519	540	540	525
R^{2-}	514–515	525	525	515
Erythrosin, HR^-	530	545	545	530
R^{2-}	525	532	533	525

The results for eosin and erythrosin are exemplified in Figures 6 and 7.

According to the main extrathermodynamic assumption, taken as a basis for studying tautomerism [24, 26–29, 67–76, 78–80, 85] and being confirmed by numerous published data [40, 55, 86–90], the spectra of species of types (**3**) and

(**5**) (Scheme 1) for the given dye are similar, and the ε_{max} values may be taken as equal. The same is the case for the species of types (**2**) and (**1**).

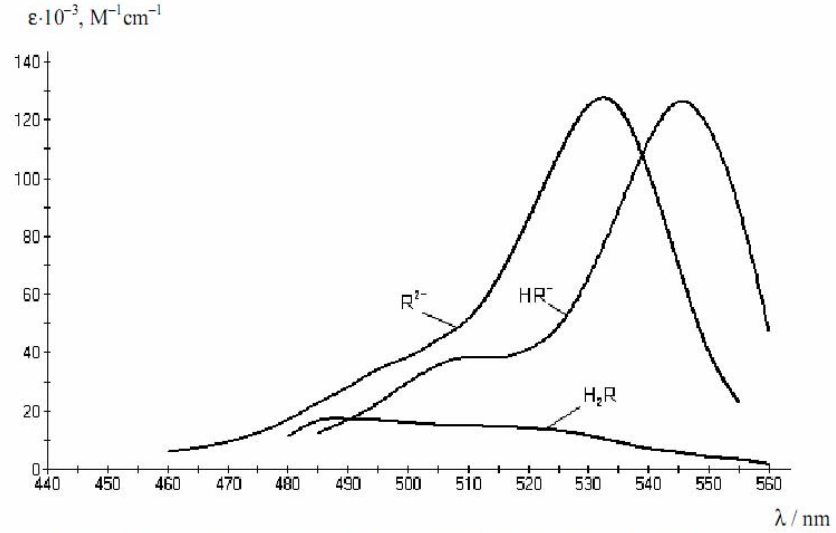

Figure 6. The absorption spectra of the equilibrium forms of erythrosin in the CTAB-based microemulsion.

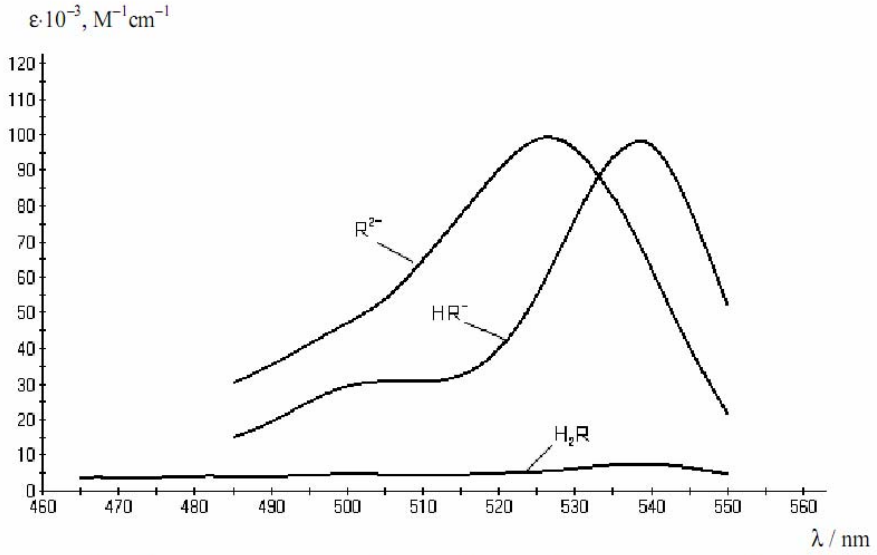

Figure 7. The absorption spectra of the equilibrium forms of eosin in the TW 80-based microemulsion.

The ionization of the carboxylic group in the 2′ position (COOH → COO^-) seriously affects only the charged xanthene chromophore, leading to blue shift of species (**7**) band as compared with the tautomer (**6**) band [24, 26–29, 67–71, 74, 91]. This experimental fact was confirmed by quantum-chemical calculations [92].

Hence, monoanions HR^- of eosin and erythrosin exist in microemulsions (Figs. 6 and 7) as tautomers (**6b**) and (**6c**), correspondingly, whereas the HR^- ion of fluorescein (Figs. 3–5) exists as tautomer (**5a**), like in other liquid media studied earlier. This is in agreement with sharp increase in the acidity of hydroxyl groups in the presence of two *ortho*-halogen subsituents. Really, from Figure 1 it follows: $K_{T_x} = k_{1,OH} / k_{1,COOH}$. For unsubstituted fluorescein in water, $pk_{1,OH}$ = 6.3, $pk_{1,COOH}$ = 3.5, hence K_{T_x} = 0.0016. In the case of eosin in water, $pk_{1,OH}$ = 2.4, $pk_{1,COOH}$ ≈ 3.5, and K_{T_x} ≈ 12.

For fluorescein molecules H_2R in microemulsions, the total decrease in absorptivity as compared with the spectrum in water (where $\varepsilon = 13.9\times10^3$ at 437 nm and $\varepsilon = 3\times10^3$ to 4×10^3 within the range of 470–485 nm) and the disappearance of the band with λ_{max} near 440 nm (Fig. 8) indicate a distinct shift of tautomeric equilibrium towards the colorless lactone (**4a**) accompanied by absence of zwitter-ion (**2a**), just as in micellar systems [24, 26–29, 71–74], solutions of dendrimers [75], cyclodextrins [78], calixarenes [79, 80], and in organic solvents [24, 27, 67, 68, 70].

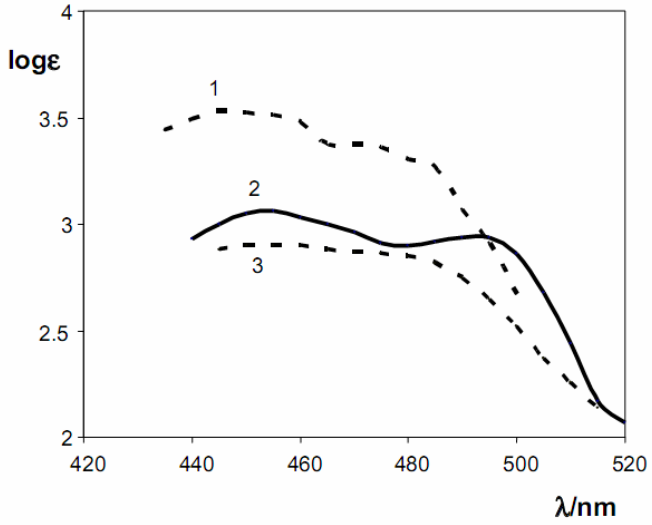

Figure 8. Absorption spectra of molecular form, H_2R, of fluorescein in SDS-based (1), in CTAB-based (2) and in TW 80-based (3) microemulsions; φ = 1.3 %, C_{HCl} = 2–4 M.

Taking ε_{max} of tautomer (**3a**) equal to that of the ion HR^- (**5a**), one can estimate fractions ('populations') of tautomers, α. For instance, in cationic microemulsions, these values are as follows: $\alpha_{3a} = \varepsilon_{max}(H_2R)/\varepsilon_{max}(HR^-) = 0.033$, $\alpha_{4a} = 1 - \alpha_{3a} = 0.967$, while α_{2a} is supposed to be equal to zero (or, at least, one may assume that $\alpha_{2a} << \alpha_{3a}$). For eosin and, even more so, for erythrosin the transfer from water to organic environments does not result in such sharp drops of the fractions of quinonoid tautomers (**3b**) and (**3c**), while zwitter-ionic tautomers are not typical for 2,4,5,7-tetrahalogen derivatives at all, due to the aforementioned high acidity of hydroxyl groups: $K_T^{/} = k_{\pm,COOH}/k_{0,OH} = k_{1,COOH}/k_{1,Z}$ (Fig. 1).

Figure 9 confirms these regularities for the case of microemulsions.

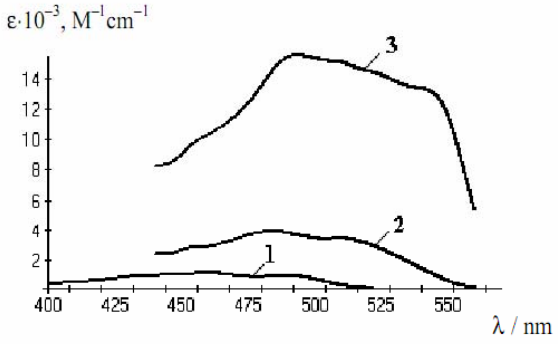

Figure 9. Absorption spectra of molecular forms, H_2R, of fluorescein (1), eosin (2), and erythrosin (3) in CTAB-based microemulsions (φ = 1.3 %, C_{HCl} = 2–4 M).

It is clear that the shifts of tautomeric equilibria result from binding of dye molecular species to the nanodroplets. However, such binding may be incomplete. And really, the molar absorptivities of the form H_2R of fluorescein in non-ionic TW 80-based and anionic SDS-based microemulsion at $\varphi = 0.026$ are correspondingly 1.57 and 1.96 times lower than those at $\varphi = 0.013$. Contrary to it, in the case of cationic CTAB-based microemulsions the ε_{H_2R} values stay constant at different φ values. On the one hand, it is reasonable to suppose that only in the last case the binding is practically complete, while in the first two dispersed systems some of molecular species are still present in the bulk (aqueous) phase to certain extent. On the other hand, variations of φ values are known to cause size changes of microdroplets in some cases [14, 20–22].

3.4. Completeness of binding of different dye species to the microdroplets

In the most cases, the pK_a^{app} values differ substantially from the 'aqueous' pK_a s (Table 1). This gives evidence for association of the dyes with the organic droplets, though the completeness of the binding of the dye species to the pseudophase may be different. The conclusions concerning the state of the dyes in the colloidal systems may also be made using the comparison of the absorption and emission spectra in water with those at various φ values.

In cationic microemulsion, the anions R^{2-} and HR^- of all the three dyes are bond by positively charged microdroplets thanks to the electrostatic attraction, whereas the neutral species H_2R are solubilized due to their low solubility in the bulk water. Only in the case of the fluorescein cationic form, the electrostatic repulsion probably hinders complete binding. The batochromic shift of the absorption bands of anions against the position in water is 7 to 22 nm (Table 2). Briefly, all the species of the three dyes studied are practically completely bound to cationic microemulsions, the single exception being the cationic species H_3R^+ (**1**). The last-named are observed at appropriate acidity only for fluorescein (**1a**). For eosin and erythrosin, the species H_3R^+ (**1b**, **1c**) appear at much higher acidity, than that for fluorescein (**1a**), and therefore for these two dyes the equilibrium (1) is not studied here at all.

In anionic microemulsions, the bands of anionic species display but modest shifts, whereas the batochromic shift for the fluorescein cation reaches 8 nm. In non-ionic dispersions, the band positions of ions coincide with those in CTAB-based ones, with a sole exception of the fluorescein R^{2-} species. The latter is most hydrophilic among the three dianions, and its band with $\lambda_{max} = 490$ nm is like that in water.

Both absorption and emission spectra of R^{2-} dianion of fluorescein in anionic and non-ionic microemulsions, at various φ, stays unchanged as compared with those in water ($\lambda_{max}^{em} = 515$ nm). Hence, the dianion **7a** stays essentially in the aqueous phase. The pK_{a2}^{app} value of fluorescein in anionic microemulsion (6.62) is very close to that in water at the same I value (6.55), which allows to conclude that the monoanion HR^- (**5a**) is also practically not bound to the pseudophase. The pK_{a2}^{app} value of the dye in non-ionic microemulsion (7.08) is somewhat higher, which allows expecting the binding of a small fraction of (**5a**) ions to nanodroplets.

The emission spectrum of R^{2-} dianion of eosin in water changes negligibly in the presence of anionic nanodroplets, the same is the situation with the absorption spectrum (Table 2). However, absorption spectrum of monoanion HR^- (**6b**) changes markedly in both anionic and non-ionic microemulsions as compared with that in water (Table 2). Hence, the expressed difference of pK_{a2}^{app}

values of eosin in these systems (5.15 and 6.17, correspondingly) and in water at I = 0.05 M (3.50) is caused by transfer of (**6b**) species into the pseudophase. Moreover, the dianion (**7b**) is partly bound.

Figure 10 demonstrates the influence of binding by the pseudophase on the dianions R^{2-} fluorescence spectra.

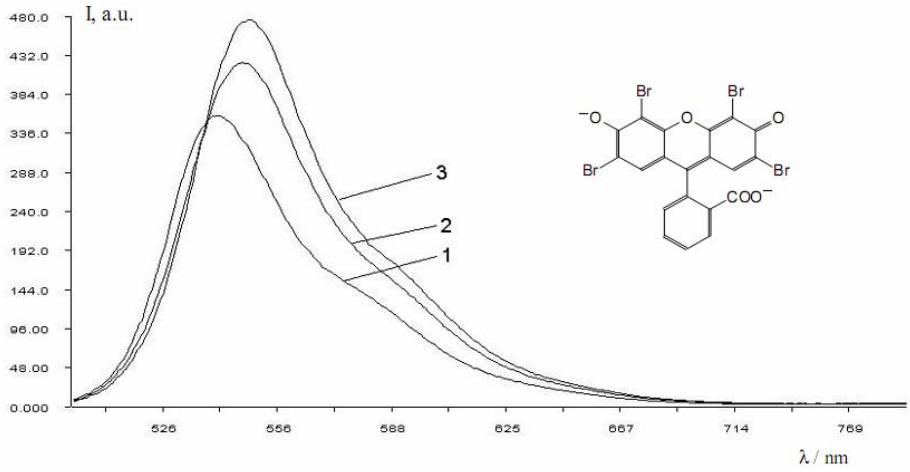

Figure 10. Fluorescence spectra of R^{2-} ion of eosin in water (1) and in non-ionic microemulsions (benzene – n-$C_5H_{11}OH$ –TW 80) at φ = 0.013 (2) and φ =0.026 (3); $C_{dye} = 3.56 \times 10^{-6}$ M.

It must be noted that further increase in φ values results in such strong changes both in the character of nanodroplets and in the structure of aqueous phase, that alterations in emission spectra may reflect not only the degree of binding.

3.5. The medium effects and the ionization microconstants

The medium effects for the pK_a^{app} values of fluorescein and eosin are gathered in Table 3. Some of them were qualitatively discussed above in terms of complete or incomplete binding. In some cases, however, the pK_a^{app} s undergo different changes as compared with the corresponding pK_a^w s even under conditions of practically complete binding of the dye species.

Such differentiating influence of non-aqueous media on the acid-base properties of the dissolved (solubilized) compounds is typical for surfactant micelles and was previously discussed in full [24–29, 71, 74–76].

Table 3. The medium effects on the indices of the ionization constants of fluorescein and eosin in microemulsions; φ = 0.013, I = 0.05 M, 25 °C

Dye/ ΔpK_a^{app}	The values of $\Delta pK_a^{app} = pK_a^{app} - pK_a^{w}$ in microemulsions:		
	in CTAB-based	in TW 80-based	in SDS-based
Fluorescein, ΔpK_{a0}^{app} =	–2.17	–1.83	+0.47
ΔpK_{a1}^{app} =	+0.04	+2.04	+1.08
ΔpK_{a2}^{app} =	–1.18	+0.28	+0.12
Eosin, ΔpK_{a1}^{app} =	–1.57	+0.83	+0.76
ΔpK_{a2}^{app} =	–0.06	+2.42	+1.40

[a] *In accord with [Eq. (6)], the thermodynamic pK_a^w values are used in calculations: pK_{a0}^w = 2.14, pK_{a1}^w = 4.45, and pK_{a2}^w = 6.80 for fluorescein and pK_{a1}^w = 2.81 and pK_{a2}^w = 3.75 for eosin.*

This demands a more circumstantial consideration of the protolytic equilibria. From the detailed ionization scheme (Fig. 1), following general equations can be derived:

$$pK_{a0} = pk_{0,OH} - \log\left(1 + K_T + K_T^{/}\right) = pk_{\pm,COOH} - \log\{1 + K_T^{//} + (K_T^{/})^{-1}\}; \quad (10)$$

$$\begin{aligned} pK_{a1} &= pk_{1,COOH} + \log\left(1 + K_T + K_T^{/}\right) - \log(1 + K_{T_x}) \\ &= pk_{1,Z} + \log\{1 + K_T^{//} + (K_T^{/})^{-1}\} - \log\left(1 + K_{T_x}\right) \\ &= pk_{1,OH} + \log\left(1 + K_T + K_T^{/}\right) - \log(1 + K_{T_x}^{-1}); \end{aligned} \quad (11)$$

$$pK_{a2} = pk_{2,COOH} + \log(1 + K_{T_x}^{-1}) = pk_{2,OH} + \log(1 + K_{T_x}); \quad (12)$$

The equations can be simplified taking into account that the K_{T_x} value is extremely low for fluorescein and high for eosin and erythrosin, and that $(1 + K_T + K_T^{/})$ equals to α_3^{-1}. Namely, for fluorescein it is useful to express the pK_a values as follows:

$$pK_{a0} = pk_{0,OH} + \log \alpha_{3a}; \quad (13)$$

$$pK_{a1} = pk_{1,COOH} - \log \alpha_{3a}; \quad (14)$$

$$pK_{a2} = pk_{2,OH}, \quad (15)$$

whereas for eosin and erythrosin:

$$pK_{a1} = pk_{1,OH} - \log \alpha_{3b,c}; \quad (16)$$

$$pK_{a2} = pk_{2,COOH}. \quad (17)$$

Now, the analysis of the medium effects in microemulsions, ΔpK_a^{app}, presented in Table 3, consists in considering the microscopic ionization constants, pk, and the corresponding Δpk values.

Also, it is worthwhile to regard the data obtained in microemulsions for some model compounds with a more simple ionization scheme (Fig. 11).

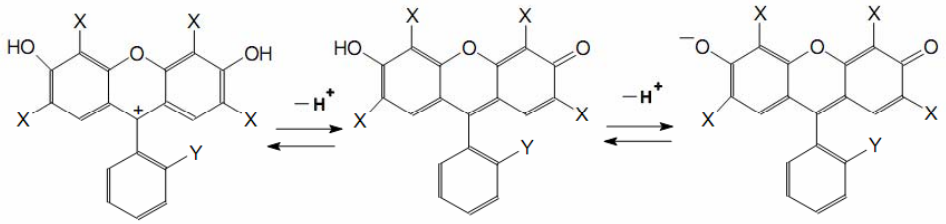

H_2R^+ HR R^-

Figure 11. Protolytic conversions of sulfonefluorescein (X = H, Y = SO_3^-), 6-hydroxy-9-phenyl fluorone (X = H, Y = H), ethyl fluorescein (X = H, Y = $COOC_2H_5$), n-decyl fluorescein (X = H, Y = COO-n-$C_{10}H_{21}$), ethyl eosin (X = Br, Y = $COOC_2H_5$), and n-decyl eosin (X = Br, Y = COO-n-$C_{10}H_{21}$).

For fluorescein in cationic microemulsions, $K_T = 29$; $pk_{0,OH} = 1.45$; $pk_{1,COOH} = 3.01$; $pk_{2,OH} = 5.62$. The latter value coincides with the $pK_{a2}^{app} = pk_{2,OH} = 5.65$ value of sulfonefluorescein at the same bulk ionic strength in analogous cationic microemulsion [21]. (The sole difference consists in using of CPC instead of CTAB.) The $pK_{a1}^{app} = pk_{1,OH}$ values of 6-hydroxy-9-phenyl fluorone, ethyl fluorescein, and *n*-decyl fluorescein in the same system are lower: 5.04, 5.15, and 5.28 respectively [21]. This should be ascribed to the influence of the additional negative charge of the COO^- or SO_3^- groups in the case of fluorescein and sulfonefluorescein, in line with the Bjerrum–Kirkwood–Westheimer concept [24, 68, 71].

The $pk_{0,OH}$ values of 6-hydroxy-9-phenyl fluorone, ethyl fluorescein, and *n*-decyl fluorescein are equal to 1.70, 1.13, and 0.94 respectively [21]. In the last case, the long hydrophobic hydrocarbon chain ensures complete binding of the dye cation to the positively charged surface, and the decrease in $pk_{0,OH}$ as compared to the 'aqueous' value of the three last-named dyes and fluorescein (3.1) is more expressed, in accordance with Eq. (6). The $pk_{0,OH} = 1.45$ and hence $\Delta pk_{0,OH} = -1.65$ values of unsubstituted fluorescein (Y = COOH) are in-between those of model compounds with Y = H and Y = $COOC_2H_5$.

The $\Delta pk_{1,COOH} = -0.48$ value of fluorescein markedly differs from $\Delta pk_{2,OH} = -1.18$. This phenomenon is numerously repeated in all the afore-cited papers of our group and should be explained in terms of the γ_i values [Eq. (6)]: the increase in the pK_a values of carboxylic acids on going from water to non-aqueous environments is more pronounced as compared with that of phenols [68]. This effect may in some cases even overcome the negative contribution of the $-\Psi/59$ term in Eq.(6). Another reason for the positive ΔpK_{a1}^{app} value of fluorescein in the cationic microemulsion is the rise in α_{4a}: 0.967 against 0.670 in water.

For eosin in cationic microemulsions, $pk_{1,OH} = -1.65$; this value agrees semi-quantitatively with those for model compounds, ethyl and *n*-decyl eosin, in CPC-based microemulsions: $pk_{1,OH} = -1.2$ to -1.3 [21]. The $\Delta pk_{2,COOH} = -0.06$ value for eosin is much less negative, in accordance with the above-mentioned peculiarity of the behavior of the carboxylic group on going from water to organic environment. Note, that all the Δpk s are estimated in respect to the thermodynamic values in water. This $\Delta pk_{2,COOH}$ value is also less negative as compared with that of $\Delta pk_{1,COOH}$ (see above), because other things being equal the strength of the anionic acids decreases more noticeably as compared with that of the neutral ones [24, 25].

The increase in the bulk ionic strength results in the rise of the pK_a^{app} s, owing to the shielding of the surface charge of the CTAB-based pseudophase. For fluorescein, the pK_{a1}^{app} and pK_{a2}^{app} are 5.84 and 6.50 respectively at 1 M KCl [26]; the $pK_{a0}^{app} = -0.07$ value [26] is practically the same as at $I = 0.05$ M, because the cationic form H_3R^+ is evidently still located in the bulk, whereas the H_2R form is uncharged. Only in CTAB micellar solutions at 4 M KCl, $pK_{a0}^{app} = 0.60$, $pK_{a1}^{app} = 6.41$, and $pK_{a2}^{app} = 7.17$ [71].

For eosin, the regularities are quite similar. Here, the pK_{a1}^{app} and pK_{a2}^{app} values in cationic microemulsions at 1 M KCl and cationic micelles at 4 M KCl are 1.74 and 5.27 [26] and 1.83 and 5.76 [71] respectively.

Earlier, Kibblewhite *et al.* [54] reported the pK_a^{app} values for lipoidal

derivatives of fluorescein and eosin, fixed in micelles of cationic, anionic, and non-ionic surfactants. The long hydrocarbon chain in the 4′-position of the phthalic acid residue ensures complete binding of all the dyes species by any kind of pseudophase. For cationic micelles both at low and high ionic strength the results are rather close to ours. A detailed comparison is hindered by the difference of the *I* values.

For anionic micelles some data for completely bound lipoidal dyes markedly differ from ours. So, for fluorescein in SDS-based microemulsions, $pK_{a0}^{app} = 2.61$, $pK_{a1}^{app} = 5.53$, and $pK_{a2}^{app} = 6.62$ (Table 1), while for the lipoidal fluorescein in SDS micelles at low ionic strength $pK_{a0}^{app} = 3.98$, $pK_{a1}^{app} = 5.97$, and $pK_{a2}^{app} = 8.84$ [54]. The last high pK_{a2}^{app} value reflects the binding of the HR^- and R^{2-} species to the negatively charged surface: the $-\Psi/59$ item in Eq. (6) makes a substantial contribution in this case. Correspondingly, the $pK_{a1}^{app} =$ 8.52 value of *n*-decyl fluorescein (Fig. 11) in SDS-based microemulsion at *I* = 0.05 M [21] is also high.

5. Conclusions

The present work was devoted to protolytic equilibria of three common hydroxyxanthene luminophores, fluorescein, eosin, and erythrosin, in direct 'benzene-in-water' microemulsions stabilized by pentanol-1 and surfactants: cationic (CTAB), anionic (SDS), and non-ionic (Tween 80). The vis-absorption spectra of dye species and 'apparent' ionization constants (twenty one values) were determined at volume fraction of the dispersed phase $\varphi = 0.013$ and bulk ionic strength I = 0.05 M (KCl + buffer). Conclusions concerning tautomerism of the molecular and ionic species were deduced from the spectral data.

The strong differentiating influence of the dispersed phase of microemulsions of different types on the acid-base properties of dyes was explained in terms of shifts of tautomeric equilibrium, specificity of microenvironmental effects, and selective binding of various dye species to the microdroplets.

Concluding, the examined microemulsions affect the complicated protolytic equilibria of the dissolved hydroxyxanthene dyes practically in the same manner as those of simple indicators studied earlier [21, 25].

References

1. *Organized Solutions. Surfactants in Science and Technology*, eds. S.E. Friberg, B. Lindman, Marcel Dekker, Inc.: N. Y., 1992.
2. Berthod, A; Garcia-Alvarez-Coque, C. *Micellar Liquid Chromatography*. Marcel Dekker, Inc.: N.Y.–Basel, 2000.

3. Shtykov, S.N. *Zh. Anal. Khim.*, **2002**, *57*, 1018–1028.
4. Pallavicini, P.; Diaz-Fernandez, Y.A.; Foti, F.; Mangano, C.; Patroni, S. *Chem. Eur. J.*, **2007**, *13*, 178–187.
5. Holmberg, K. *Eur. J. Org. Chem.*, **2007**, 731–742.
6. Khan, M.N. *Micellar Catalysis*. CRC Press: Boca Raton, 2007.
7. Popov, A. F. *Pure Appl. Chem.*, **2008**, *80*, 1381–1397.
8. Onel, L.; Buurma, N.J. *Annu. Rep. Prog. Chem., Sect. B.*, **2009**, *105*, 363–379.
9. Pallavicini, P.; Diaz-Fernandez, Y.A.; Pasotti, L. *Coord. Chem. Rev.*, **2009**, *253*, 2226–2240.
10. Gainanova, G. A.; Vagapova, G. I.; Syakaev, V. V.; Ibragimova, A. R.; Valeeva, F. G.; Tudriy, E. V.; Galkina, I. V.; Kataeva, O. N.; Zakharova, L. Ya.; Latypov, Sh. K.; Konovalov, A. I. *J. Coll. Int. Sci.* **2012**, *367*, 327–336.
11. Karpichev, Y.; Matondo, H.; Kapitanov, I.; Savsunenko, O.; Vendrenne, M.; Poinsot, V.; Rico-Lattes, I.; Lattes, A. *Cent. Eur. J. Chem.*, **2012**, *10*, 1059–1065.
12. Manet, S.; Karpichev, Y.; Dedovets, D.; Oda, R. *Langmuir* **2013**, *29*, 3518–3526.
13. Mchedlov-Petrossyan, N. O.; Vodolazkaya, N. A.; Kamneva, N. N. Acid-base equilibrium in aqueous micellar solutions of surfactants. In: Micelles: Structural Biochemistry, Formation and Functions & Usage, N. Y.: Nova Publishers, 2013. Chapter 1.
14. Microemulsions Structure and Dynamics, Friberg, S.E. and Bothorel, P., Eds., Boca Raton: CRC, 1987. Translated under the title Mikroemul'sii: struktura i dinamika, Moscow: Mir, 1990.
15. Letts, K.; Mackay, R. A. *Inorg. Chem*. **1975**, *14*, 2990–2993.
16. Hermansky, C.; Mackay, R. A. *J. Colloid Int. Sci.* **1980**, *73*, 324–331.
17. Mackay, R. A.; Jacobson, K.; Tourian, J. *J. Colloid Int. Sci.* **1980**, *76*, 515–524.
18. Mackay, R. A. *Adv. Colloid Int. Sci.* **1981**, *15*, 131–156.
19. Berthod, A.; Saliba, C. *Analusis* **1986**, *14*, 414–420.
20. Mchedlov-Petrosyan, N. O.; Isaenko, Yu. V.; Tychina, O. N. *Zh. Obshch. Khim.* **2000**, *70*, 1963–1971.
21. Mchedlov-Petrossyan, N. O.; Isaenko, Yu. V.; Salamanova, N. V.; Alekseeva, V. I.; Savvina, L. P. *Zh. Anal. Khim.* **2003**, *58*, 1140–1154.
22. Mchedlov-Petrossyan, N. O.; Isaenko, Yu. V.; Goga, S. T. *Zh. Obshch. Khim*. **2004**, *74*, 1871–1877.
23. Mchedlov-Petrossyan, N. O.; Vodolazkaya, N. A.; Timiy, A. V.;

Gluzman, E. M.; Alekseeva, V. I.; Savvina, L. P. http://preprint.chemweb.com/physchem/0307002.
24. Mchedlov-Petrossyan, N. O. *Differentiation of the Strength of Organic Acids in True and Organized Solutions*, Kharkov National University Press: Kharkov, 2004.
25. Mchedlov-Petrossyan, N. O. *Pure Appl. Chem*. **2008**, *80*, 1459–1510.
26. Vodolazkaya, N. A.; Gurina, Yu. A.; Salamanova, N. V.; Mchedlov-Petrossyan, N. O. *J. Mol. Liquids* **2009**, *145*, 188–196.
27. Mchedlov-Petrossyan, N. O.; Vodolazkaya, N. A.; Gurina, Yu. A.; Sun, W-C.; Gee, K. R. *J. Phys. Chem. B* **2010**, *114*, 4551–4564.
28. Vodolazkaya, N. A.; Mchedlov-Petrossyan, N. O.; Salamanova, N. V.; Surov, Yu.N.; Doroshenko, A. O. *J. Mol. Liquids* **2010**, *157*, 105–112.
29. Vodolazkaya, N. A.; Kleshchevnikova, Yu. A.; Mchedlov-Petrossyan, N. O. *J. Mol. Liquids* **2013**, *187*, 381–388.
30. Choi, M. F.; Hawkins, P. *J. Chem. Soc., Faraday Trans.* **1995**, *91*, 881–885.
31. Choi, M.F.; Hawkins, P. *Sensors and Actuators. B.* **1997**, *39*, 390–394.
32. Choi, M.M.F. *J. Photochem. Photobiol. A* **1998**, *114*, 235–239.
33. Chan, M. A.; Lam, S. K.; Lo, D. *J. Fluoresc*. **2003**, *12*, 327–332.
34. Bailey, R. T.; Cruickshank, F. R.; Deans, G.; Gillanders, R. N.; Tedford, M. C. *Anal. Chim. Acta* **2003**, *487*, 101–108.
35. Fuh, M. R. S.; Burgess, L. W.; Hirschfeld, T.; Christian, G. D.; Wang, F. *Analyst* **1987**, *112*, 1159–1163.
36. Pringsheim, E.; Zimin, D.; Wolfbeis, O. S. *Adv. Mater.* **2001**, *13*, 819–822.
37. Guan, X.; Liu, X.; Su, Z.; Liu, P. *Reactive Funct. Polym.* **2006**, *66*, 1227–1239.
38. Sjöback, R.; Nygren, J.; Kubista, M. *Biopolymers* **1998**, *46*, 445–453.
39. Klonis, N.; Clayton, A. H. A.; Voss, E. W.; Sawyer, W. H. *Photochem. Photobiol*. **1998**, *67*, 500–510.
40. Klonis, N.; Sawyer, W. H. *Photochem. Photobiol.* **2003**, *77*, 502–509.
41. Yakovleva, J.; Davidsson, R.; Lobanova, A.; Bentsson, M.; Eremin, S.; Laurell, T.; Emneus, J. *Anal. Chem*. **2002**, *74*, 2994– 3004.
42. Kubica, K.; Langner, M.; Gabrielska, J. *Cellular a. Molecular Biol. Lett*. **2003**, *8*, 943–954.
43. Slyusareva, E. A.; Gerasimov, M. A.; Sizykh, A. G.; Gornostaev, L. M. *Russ. Phys. J*. **2011**, *54*, 485–492.
44. Yadav, R.; Das, S.; Sen, P. *Austr. J. Chem*. **2012**, *65*, 1305–1313.
45. Efron, N. *Clin. Exp. Optom.* **2013**, *96*, 400–421.

46. Gerke, K. M.; Sidle, R. C.; Mallants, D. *J. Hydrol. Hydromech.* **2013**, *61*, 313–325.
47. Zhang, F.; Shi, F.; Ma, W.; Gao, F.; Jiao, Y.; Li, H.; Wang, J.; Shan, Z.; Lu, X.; Meng, S. *J. Phys. Chem. C* **2013**, *117*, 14659–14666.
48. Nagarajan, N.; Paramaguru, G.; Vanitha, G.; Renganathan, R. *J. Chem. (Hidwani Publ. Corp.)* **2013**, Article ID 585920, 7 pages.
49. Hahn, U.; Gorka, M.; Vögtle, F.; Vicinelli, V.; Ceroni, P.; Maestri, M.; Balzani, V. *Angew. Chem. Int. Ed.* **2002**, *41*, 3595–3598.
50. Marchioni, F.; Venturi, M.; Credi, A.; Balzani, V.; Belohradsky, M.; Elizarov, A. M.; Tseng, H.-R.; Stoddart, J. F. *J. Amer. Chem. Soc*. **2004**, *126*, 568–573.
51. Li, J. J.; Fang, X.; Tan, W. *Biochem. Biophys. Res. Comm*. **2002**, *292*, 31–40.
52. Kojima, H.; Urano, Y.; Kikuchi, K.; Higuchi, T.; Hirata, Y.; Nagano, T. *Angew. Chem. Int. Ed.* **1999**, *38*, 3209–3212.
53. Nagano, T.; Yoshimura, T. *Chem. Rev.* **2002**, *102*, 1235–1269; and references cited therein.
54. Kibblewhite, J.; Drummond, C. J.; Grieser, F.; Thistlethwaite, P. J. *J. Phys. Chem.* **1989**, *93*, 7464–7473.
55. Song, A.; Zhang, J.; Zhang, M.; Shen, T.; Tang, J. *Coll. Surf. A* **2000**, *167*, 253–262.
56. Pellosi, D. S; Estevão, B. M; Semensato, J.; Severino, D.; Baptista, M. S.; Politi, M.J.; Hioka, N.; Caetano, W. *J. Photochem. Photobiol. A.* **2012**, *247*, 8–15.
57. Pellosi D. S.; Estevão, B. M.; Freitas, C. F.; Tsubone, T. M.; Caetano, W.; Hioka, N. *Dyes Pigments* **2013**, *99*, 705–712.
58. Brown, L.; Halling, P. J.; Johnston, G. A.; Suckling, C. J.; Valivety, R. H. *J. Chem. Soc., Perkin Trans. 1* **1990**, 3349–3353.
59. Halling, P. J.; Han, Y.; Johnston, G. A.; Suckling, C. J.; Valivety, R. H. *J. Chem. Soc., Perkin Trans. 2* **1995**, 911–918.
60. Loginova, L. P.; Samokhina, L. V.; Mchedlov-Petrossyan, N. O.; Alekseeva, V. I.; Savvina, L. P. *Colloids Surf. A*. **2001**, *193*, 207–219.
61. Schröder, C. R.; Weidgans, B. M.; Klimant, I. *Analyst* **2005**, *130*, 907–916.
62. Zhanga, X.-F.; Liub, Q.; Wang, H.; Fua, Z.; Zhang, F. *J. Photochem. Photobiol. A* **2008**, *200*, 307–313.
63. Hu, J.; Zhang, X.; Wang, D.; Hu, X.; Liu, T.; Zhang, G.; Liu, S. *J. Mater. Chem*. **2011**, *21*, 19030 – 19038.
64. Huang, S. T.; Shi, Y.; Li, N. B.; Luo, H. Q. *Chem. Comm.* **2011**, *48*,

747–749.
65. Choi, M. F.; Hawkins, P. *Spectrosc. Lett.* **1994**, *27*, 1049–1063.
66. Magde, D.; Rojas, G.; Seybold, P. *Photochem. Photobiol.* **1999**, *70*, 737–744.
67. Mchedlov-Petrossyan, N. O.; Tychina, O. N.; Berezhnaya, T. A.; Alekseeva, V. I.; Savvina, L. P. *Dyes Pigments* **1999**, *43*, 33–46.
68. Mchedlov-Petrossyan, N. O.; Kukhtik, V. I.; Bezugliy V. D. *J. Phys. Org. Chem.* **2003**, *16*, 380–397.
69. Mchedlov-Petrossyan, N. O.; Vodolazkaya, N. A.; Surov, Yu. N.; Samoylov, D. V. *Spectrochim. Acta A* **2005**, *61*, 2747–2760.
70. Mchedlov-Petrossyan, N. O.; Vodolazkaya, N. A.; Salamanova, N. V.; Roshal, A. D.; Filatov, D. Yu. *Chemistry Lett.* **2010**, *39,* 30–31.
71. Mchedlov-Petrossyan, N. O.; Kleshchevnikova, V. N. *J. Chem. Soc., Faraday Trans.* **1994**, *90*; 629–640.
72. Mchedlov–Petrossyan, N. O.; Timiy, A. V.; Vodolazkaya, N. A. http://preprint.chemweb. com/physchem/0203011.
73. Mchedlov-Petrossyan, N. O.; Isaenko Y. V.; Vodolazkaya, N. A.; Goga, S. T. http://preprint.chemweb.com/physchem/0309005.
74. Vodolazkaya, N. A.; Shakhova, P. V.; Mchedlov-Petrossyan, N. O. *Zh. Obshch. Khim*. **2009**, *79*, 1081–1089.
75. Mchedlov-Petrossyan, N. O.; Bryleva, E. Yu.; Vodolazkaya, N. A.; Dissanayake, A. A.; Ford, W.T. *Langmuir* **2008**, *24*, 5689–5699.
76. Bryleva, E. Yu.; Vodolazkaya, N .A.; Mchedlov-Petrossyan, N. O.; Samokhina, L. V.; Matveevskaya, N. A.; Tolmachev, A. V. *J. Colloid Int. Sci*. **2007**, *316*, 712–722.
77. Bezkrovnaya, O. N.; Mchedlov-Petrossyan, N. O.; Vodolazkaya, N. A.; Alekseeva, V. I.; Savvina, L. P.; Yakubovskaya, A. G. *Zh. Prikl. Khim*. **2008**, *81*, 659–666.
78. Bogdanova, L. N.; Mchedlov-Petrossyan, N. O.; Vodolazkaya, N. A.; Lebed, A. V. *Carbohydr. Res*. **2010**, *345*, 1882–1890.
79. Cheipesh, T. A.; Mchedlov-Petrossyan, N. O.; Zagorulko, E. S.; Rodik, R. V.; Kalchenko, V. I. *Dopovidi NAN Ukrainy*, **2013**, no. 12, 131–138.
80. Cheipesh, T. A.; Zagorulko, E. S.; Mchedlov-Petrossyan, N. O.; Rodik, R. V.; Kalchenko, V. I. *J. Mol. Liquids* **2014**, *193*, 232–238.
81. Mchedlov-Petrossyan, N. O.; Vodolazkaya, N. A.; Yakubovskaya, A. G.; Grigorovich, A. V.; Alekseeva, V. I.; Savvina, L. P. *J. Phys. Org. Chem.* **2007**, *20*, 332–344.
82. http://www-chemo.univer.kharkov.ua/kholin/clinp.html
83. Salamanova, N. V.; Vodolazkaya, N. A.; Mchedlov-Petrossyan, N. O.

Kharkov University Bull. **2003**, no. 596, Chemistry, issue 10 (33), 137–141.
84. Nikiforova, E. M.; Bryleva, E. Yu.; Mchedlov-Petrossyan, N. O. *Zh. Fiz. Khim.* **2008**, *82*, 1614–1618.
85. Mchedlov-Petrossyan, N. O. *Zh. Anal. Khim.* **1979**, *34*, 1055–1059.
86. Chen, S. C.; Nakamura, H.; Tamura, Z. *Chem. Pharm. Bull.* **1979**, *27*, 475–479.
87. Zhao, Z. G.; Shen, T.; Xu, H.-J. *Spectrochim. Acta. 1989*, 45 A, 1113–1116.
88. Amat-Guerri, F.; Lopez-Gonzalez, M. M. C.; Sastre, R.; Martinez-Utrilla, R. *Dyes Pigments* **1990**, *13*, 219–232.
89. Klonis, N.; Sawyer, W. H. *J. Fluoresc.* **1996**, *6*, 147–157.
90. Orte, A.; Crovetto, L.; Talavera, E. M.; Boens, N.; Alvarez-Pez, J. M. *J. Phys. Chem. A.* **2005**, *109*, 734–747.
91. Mchedlov-Petrossyan, N. O.; Salamanova N. V.; Vodolazkaya, N. A.; Gurina, Yu. A.; Borodenko, V. I. *J. Phys. Org. Chem.* **2006**, 19, 365–375.
92. Mchedlov-Petrossyan, N. O.; Ivanov, V. V. *Zh. Fiz. Khim.* **2007**, *81*, 117–121.